

Quantum Tunneling of the Magnetization in Systems with Anisotropic 4f Ion Pairs: Rates from Low-Temperature Zero-Field Relaxation

Thomas Greber*

Cite This: <https://doi.org/10.1021/acsomega.4c04388>

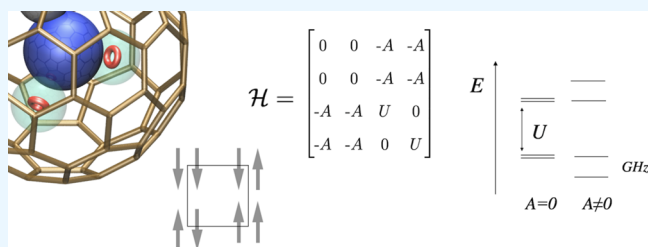
Read Online

ACCESS |

Metrics & More

Article Recommendations

ABSTRACT: Anisotropic open shell 4f ions have magnetic moments that can be read and written as atomic bits. If it comes to quantum applications where the phase of the wave function has to be written, controlled, and read, it is advantageous to rely on more than one atom that carries the quantum information on the system because states with different susceptibilities may be addressed. Such systems are realized for pairs of lanthanides in single-molecule magnets, where four pseudospin states are found and mixed in quantum tunneling processes. For the case of endohedral fullerenes like Dy₂S@C₈₂ or Tb₂ScN@C₈₀, the quantum tunneling of the magnetization is imprinted in the magnetization lifetimes at sub-Kelvin temperatures. A (4 × 4) Hamiltonian that includes quantum tunneling of the magnetization and the dipole and exchange interaction between the two lanthanide magnetic moments predicts the lifting of the zero-field ground state degeneracy and nonlinear coupling to magnetic fields in such systems.



INTRODUCTION

Since the description of the covalent molecular bond in the hydrogen molecule by Heitler and London,¹ the concept of hybridization established as a central consequence of quantum mechanics. Hybridization also imposes state separation of ammonia NH₃ ground states from a superposition of the two possibilities of placing the nitrogen atom above or below the H₃ plane, leading to the demonstration of stimulated microwave emission and manifested coherent light-matter interaction.² Furthermore, magnetic moments or spins can be changed upon level crossing in a coherent fashion,³ where such quantum tunneling of the magnetization survives as well in mesoscopic systems like crystals of single-molecule magnets (SMMs).⁴

SMMs feature bistable spin configurations with lifetimes in the order of seconds or longer⁵ and the search for the best systems proceeds via the investigation of ensembles of SMMs. In early sub-Kelvin magnetization measurements of dilute holmium ions in ionic crystals, which behave like single ion molecular magnets, it was found that nuclear spins affect the relaxation of the magnetization.⁶ This is also reflected in sub-Kelvin specific heat experiments on SMMs with more than one atom forming the magnetic cores of the molecules.⁷ Such preludes were the starting point for the understanding of the magnetic relaxation of molecular magnets.⁸ Today predictions on the magnetic relaxation times and the quantum tunneling of the magnetization are made for single ion systems.⁹ Be that as it may, eventually it is desirable to maintain and control coherence in SMMs possibly with electromagnetic radiation.

Lanthanide double decker molecules realized first mono-nuclear complexes with SMM behavior where a 4f⁸ Tb³⁺ ion played the role of the bistable magnet.¹⁰ Single-ion SMMs further evolved and today's molecules reach hystereses above liquid nitrogen temperature.¹¹ Besides this search for highest blocking temperatures, single single-ion molecular magnets were used for read out of nuclear spin states¹² and implementation of quantum algorithms.¹³ In parallel spin control and stability on single lanthanide ions on surfaces was obtained.^{14,15}

For the roadmap to few atom quantum devices it is important to explore the interference of more than one open shell atom. In this aspect endofullerenes provide the unique opportunity of arranging up to three lanthanides in otherwise impossible very close distance (<0.4 nm), inside a magnetically quiet carbon shell.¹⁶

The ground states of axially anisotropic 4f ion pairs can be described with a pseudospin model, where the magnetic moments on the two ions may assume two orientations.^{17,18} The ligand fields lift the Hund degeneracies of the 4f ions.^{17,19,20} If they are dominated by anions like S²⁻ or N³⁻, cations like Tb³⁺, Dy³⁺, or Ho³⁺ are expected to display axial magnetic

Received: May 13, 2024

Revised: August 6, 2024

Accepted: August 7, 2024

anisotropy with a pseudospin pointing toward the anion or away from it. This is because the oblate (ring-like) high J_z orbitals imply smaller Coulomb repulsion between the anion and the 4f shell, compared to the prolate (rod-like) ones with low J_z 's.^{19,21} The term "pseudospin" is used because the ligand field splits the $2J + 1$ total angular momentum states, where for {Tb, Dy, Ho} the $J_z = \{\pm 6, \pm 15/2, \pm 8\}$ have the lowest energy. The excitation to the second lowest J_z level is large and in the order of several hundred $k_B K$,²² which allows to neglect these excitations at low temperatures.

■ STATUS QUO

Figure 1a,b display the two endofullerenes $Dy_2S@C_{82}-C_s$ and $Tb_2ScN@C_{80}-I_h$ that serve as model systems for the

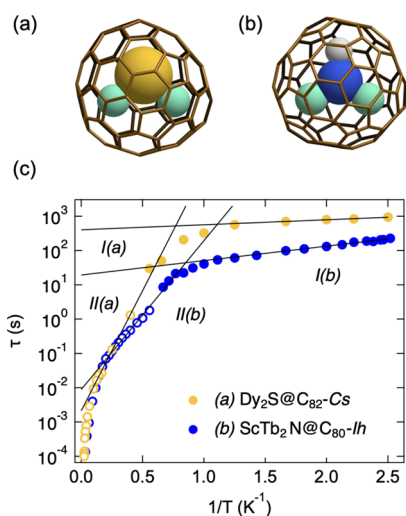


Figure 1. Dilanthanide SMMs. Model of (a) $Dy_2S@C_{82}-C_s$ and (b) $Tb_2ScN@C_{80}$. The sizes of the endohedral ions Dy or Tb (turquoise), Sc (gray), S (yellow), and N (blue) are mimicked with their ion radii. (c) Arrhenius plot of the zero-field magnetization lifetimes τ for $Dy_2S@C_{82}-C_s$ (yellow)²⁵ and $Tb_2ScN@C_{80}-I_h$ (blue).²⁶ Full symbols: DC sub-Kelvin measurements, open symbols: AC measurements. *I* and *II* indicate Arrhenius processes (see Table 1).

investigation of the quantum tunneling of the magnetization in axially anisotropic 4f ion pairs. The number of cage carbon atoms, 82 and 80, and the isomers, C_s and I_h , determine the stabilization of $(Dy_2S)^{4+23}$ and $(Tb_2ScN)^{6+24}$ endohedral units, respectively. As they do not affect the conclusions of this paper the cage isomer labels are omitted in the following.

The status quo of the understanding is a picture developed for $Dy_2ScN@C_{80}$ where the zero-field ground state splits in two time reversal symmetric doublets (TRDs).¹⁸ The splitting is reflected in the temperature dependence of the zero-field magnetization lifetime. This is an empirical observation which implies that thermal fluctuations exceeding the energy splitting accelerate the reaching of the thermal equilibrium. It is

rationalized with a coupling of the split TRDs with quasiparticles like phonons in the thermal bath. For $Dy_2S@C_{82}$ the temperature dependence of the zero-field magnetization lifetime confirmed the splitting of the two TRDs. Below 2 K the temperature dependence tended to level off, which was assigned to the onset of quantum tunneling of the magnetization.²⁵ This was not found for $Tb_2ScN@C_{80}$ but a further Arrhenius barrier was identified down to 400 mK.²⁶ It was argued that this 1 K barrier is not explained within the ground state picture in ref 18 and dipolar intermolecular interactions were offered as an explanation. Since both molecules should have similar intermolecular magnetic interactions, but as no 1 K barrier was found in $Dy_2S@C_{82}$ the intermolecular interaction hypothesis may not be the complete picture.

■ RESULTS AND DISCUSSION

In the following an explanation for the sub-Kelvin temperature dependence of the zero-field magnetization lifetime is proposed that suggests the magnitude of the coherent pseudospin tunneling rates in molecules with coupled anisotropic 4f ion pairs. Figure 1c displays the published zero-field magnetization lifetimes of $Dy_2S@C_{82}$ ²⁵ and $Tb_2ScN@C_{80}$ ²⁶ in an Arrhenius plot in the temperature range between 0.4 and 30 K. The samples had natural isotope abundance. For the extraction of characteristic excitation energies, we follow Kostanyan et al.²⁶ The solid lines represent Arrhenius barriers $\tau_0 \exp(\Delta_{\text{eff}}/k_B T)$. In Table 1 the fit-results of two distinct decay processes with barriers Δ_{eff}^i and prefactors τ_0^i ($i \in \{I, II\}$) are listed for both molecules. Process *II* in the order of 10 K is the decay that is mediated via the above-discussed TRD excitation.¹⁸ Here process *I* is assigned to the quantum tunneling of the magnetization that is shown in the following to cause a zero-field splitting of the ground state TRD.

Figure 2 sketches the model of the ground state of axially anisotropic 4f ion pairs like those in $Dy_2S@C_{82}$ or $Tb_2ScN@C_{80}$ in zero external magnetic field. The two pseudospins with a magnetic moment μ in the order of $10 \mu_B$ allow 2^2 possible ground state configurations that split by a dipole and exchange interaction U into the two TRDs ($|1\rangle, |\bar{1}\rangle$) and ($|2\rangle, |\bar{2}\rangle$).¹⁸ For the states $|1\rangle$ and $|\bar{1}\rangle$ the scalar product between the two pseudospins is positive and they are called ferromagnetically coupled, while it is negative for $|2\rangle$ and $|\bar{2}\rangle$ that are antiferromagnetically coupled. While the angle between the two pseudospin axes affects the magnetization curves,²⁷ it is not of importance for the below conclusions on the quantum tunneling of the magnetization. For $Dy_2ScN@C_{80}$, $Tb_2ScN@C_{80}$, $Dy_2S@C_{82}$ and $Dy_2TiC@C_{80}$ the ground states were found to be "ferromagnetic",^{18,25–27} while $Dy_2O@C_{82}$ has an antiferromagnetic groundstate.²⁸ The below theory is applicable for both couplings. The energy difference U was extracted from the equilibrium magnetization curves and the temperature dependence of the magnetization lifetimes^{18,25–28} without consideration of the tunneling of the magnetization.

Table 1. Fit Results of Prefactors τ_0 (s) and Barriers Δ_{eff}/k_B (K) of Two Arrhenius Processes *I* and *II* for the Temperature Dependence of the Zero-Field Magnetization Relaxation Times τ for $Dy_2S@C_{82}$ and $Tb_2ScN@C_{80}$ in Figure 1c

| | $Dy_2S@C_{82}$ | | $Tb_2ScN@C_{80}$ | |
|-----------|--------------------------------|---------------------------|--------------------------------|---------------------------|
| | τ_0 (s) | Δ_{eff}/k_B | τ_0 (s) | Δ_{eff}/k_B |
| <i>I</i> | $(4.0 \pm 0.3) \times 10^2$ | 0.34 ± 0.03 | $(1.9 \pm 0.2) \times 10^1$ | 0.97 ± 0.04 |
| <i>II</i> | $(2.1 \pm 1.3) \times 10^{-3}$ | 16.1 ± 1.1 | $(8.9 \pm 1.0) \times 10^{-3}$ | 10.0 ± 0.2 |

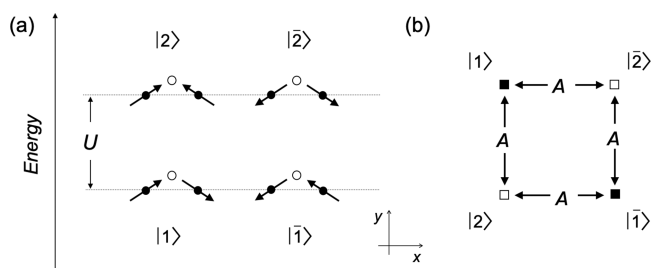


Figure 2. Pseudospin-pair ground states. (a) Pseudospin configurations for axially anisotropic 4f ion pairs. The two pseudospins on the 4f ions (black) may point toward or away from the central anion (open circle). Four states $|1\rangle$, $|\bar{1}\rangle$, $|2\rangle$ and $|\bar{2}\rangle$ may form, where $(|1\rangle, |\bar{1}\rangle)$ and $(|2\rangle, |\bar{2}\rangle)$ are TRDs with the dipole and exchange splitting U . The resulting magnetic moments of TRD1 point along $\pm x$ and those of TRD2 along $\pm y$. (b) Four states on a square in a Hilbert space. Two adjacent states (corners) are separated by the flip of one pseudospin out of the two. A is the tunneling matrix element for a pseudospin flip. The different energy (black or white) of adjacent states provided the rationale “exchange protection” for the large remanence of $\text{Dy}_2\text{ScN}@C_{80}$.¹⁸

The “Hilbert space topology” of the four states is depicted in Figure 2b. They lie on the corners of a square where the sides connect states that differ by one pseudospin flip. It was anticipated that single pseudospin flips or tunneling within the four states was inhibited by the dipole and exchange interaction U . The difference between $\text{Dy}_2\text{ScN}@C_{80}$ and $\text{Tb}_2\text{ScN}@C_{80}$ was assigned to the Kramers degeneracy of the odd $4f^9 \text{Dy}^{3+}$ ions in contrast to the even $4f^8 \text{Tb}^{3+}$ ions.^{25,26}

Without tunneling of the magnetization, the four states $|1\rangle$, $|\bar{1}\rangle$, $|2\rangle$, and $|\bar{2}\rangle$, would be eigenstates of the system, where in zero field and with ferromagnetic coupling $|1\rangle$ and $|\bar{1}\rangle$ form a 2-fold degenerate ground state. With tunneling of the magnetization the ground state degeneracy is lifted. This can be seen when the Hamiltonian \mathcal{H} for Figure 2b is written as a 4×4 matrix (eq 1) and when the eigenvalues are determined. On the diagonal we find the energies as put forward in the picture of Westerström.¹⁸ Off diagonal we find the tunneling matrix element A that describes the single spin flip probability. For the case of a single 4f ion like in $\text{DySc}_2\text{N}@C_{80}$ A is expected to be zero for an unperturbed Kramers ion without nuclear spin like $^{162}\text{Dy}^{3+}$. For coupled 4f ion pairs this must not hold because of the even number of electrons involved. Therefore, the pseudospins of 4f ion pairs couple and a nonzero A lifts degeneracies. The sign of the tunneling matrix element is chosen such that the amplitudes of the ground state $|\Phi_1\rangle$ have the same sign and we write the Hamiltonian:

$$\mathcal{H} = \begin{bmatrix} 0 & 0 & -A & -A \\ 0 & 0 & -A & -A \\ -A & -A & U & 0 \\ -A & -A & 0 & U \end{bmatrix} \quad (1)$$

where double flips $|1\rangle \leftrightarrow |\bar{1}\rangle$ or $|2\rangle \leftrightarrow |\bar{2}\rangle$ across the diagonals in Figure 2b are neglected. An arbitrary state $|\Psi\rangle$ is described by 4 amplitudes $|a_1, a_{\bar{1}}, a_2, a_{\bar{2}}\rangle$, where for example $|0, 1, 0, 0\rangle$ corresponds to $|\bar{1}\rangle$, which is for $A \neq 0$ not an eigenstate. The eigenstates are mixtures of the base in Figure 2. Importantly, the lifting of the zero-field degeneracy of the ground state should enable pseudospin control and manipulation. The four eigenvalues and the eigenvector amplitudes for $U/A = 10$ of eq 1 are listed in Table 2.

Table 2. Eigenvalues λ_i and Eigenvectors $|\Phi_i\rangle$ of the Zero-Field Hamiltonian (1) with Amplitudes a_j on the Basis of Figure 2 for a Ratio between the Dipole and Exchange Interaction and the Pseudospin Tunneling Matrix Element $U/A = 10$

| eigenvalue λ_i | $ \Phi_i\rangle$ | a_1 | $a_{\bar{1}}$ | a_2 | $a_{\bar{2}}$ |
|------------------------------|------------------|-------|---------------|-------|---------------|
| $(U - \sqrt{16A^2 + U^2})/2$ | $ \Phi_1\rangle$ | 0.69 | 0.69 | 0.13 | 0.13 |
| 0 | $ \Phi_2\rangle$ | -0.71 | 0.71 | 0 | 0 |
| U | $ \Phi_3\rangle$ | 0 | 0 | -0.71 | 0.71 |
| $(U + \sqrt{16A^2 + U^2})/2$ | $ \Phi_4\rangle$ | 0.13 | 0.13 | -0.69 | -0.69 |

Figure 3 shows the eigenvalue spectrum as a function of U/A . While U has been determined experimentally¹⁸ and theoret-

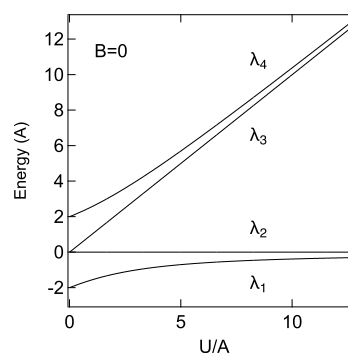


Figure 3. Eigenvalues of the 4×4 Hamiltonian (eq 1) as a function of the ratio between the dipole and exchange interaction and the pseudospin tunneling matrix element U/A in zero field ($B = 0$). The energy scale is the tunneling matrix element of the two pseudospins A .

ically,^{17,29} A was neglected so far, though it is essential for understanding and further exploitation of 4f ion pair-systems. Setting $(\lambda_2 - \lambda_1) = \Delta_{\text{eff}}^I$ we get for the two molecules frequencies Δ_{eff}^I/h of 6.3 and 20.8 GHz or temperatures $\Delta_{\text{eff}}^I/k_B$ of 0.34 and 0.97 K (Table 1), while the tunneling matrix elements A/k_B of $\text{Dy}_2\text{S}@C_{82}$ and $\text{Tb}_2\text{ScN}@C_{80}$ get 85 and 250 mK with $U/A = 190$ and 40, respectively. For Tb A is in the range of the hyperfine interaction of isolated $^{159}\text{Tb}^{3+}$ with a nuclear spin $I = 3/2$.³⁰ The hyperfine interaction influences the magnetization lifetimes of SMMs, though no strong influence on the quantum tunneling rate was found for isotope separated Dy dimer SMMs.³¹ It is therefore expected that the nuclear spin rather influences the prefactors τ_0 but not the Δ_{eff} barriers in the $\ln \tau$ vs $1/T$ data. Such a trend can be suggested from magnetization measurements down to 2 K on isotope enriched Dy single ion molecules.³² In the present case of coupled ion pairs the τ_0 prefactors of the Dy and the Tb analogues are 400 and 19 s, respectively (Table 1). This corresponds to very low attempt frequencies compared to the Δ_{eff}^I/h 's and indicates how difficult it is to predict the prefactors.

The magnetic moment of the states can be calculated from $\langle \Psi | M | \Psi \rangle$, where $M = (\vec{\mu}_1, -\vec{\mu}_1, \vec{\mu}_2, -\vec{\mu}_2)$ are the magnetic moments of the base. It is seen that all four eigenstates of Hamiltonian (1) have no magnetic moment.

In an external B-field the eigenstates may become magnetic. Hamiltonian (1) has to be complemented with corresponding Zeeman terms $E_j^Z = -\vec{\mu}_j \cdot \mathbf{B}$, where $\vec{\mu}_j$ are the magnetic moments of the four possible pseudospin configurations, and \mathbf{B} the external magnetic field. The Zeeman energies have to be added

to the diagonal elements of the Hamiltonian (1). Accordingly, the effect of the state mixing or hybridization also displays in the plot of the eigenvalues vs the applied B-field. Figure 4 shows the

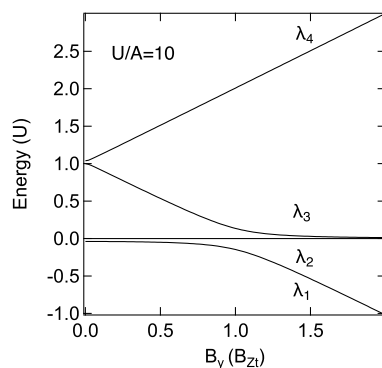


Figure 4. Eigenvalues λ_i of eq 1 with Zeeman energies as a function of an external magnetic field along y for a ratio between the dipole and exchange interaction and the pseudospin tunneling matrix element $U/A = 10$. The B-field scale is the Zeeman threshold field $B_{Zt} = U/2\mu$. The energy scale is the dipole and exchange interaction between the two pseudospins U .

case for a B-field along y , where the field scale is chosen to be the Zeeman threshold field $B_{Zt} \equiv U/2\mu$,²⁶ which is 1.9 and 1.6 T for $Dy_2S@C_{82}$ and $Tb_2ScN@C_{80}$, respectively. The eigenvector of the ground state $|\Phi_1\rangle$ for $B = 0$ without magnetic moment evolves for large fields nonlinearly to state $|2\rangle$ with a magnetization along y , while the first excited state $|\Phi_2\rangle$ remains without magnetic moment and thus constant energy.

Of course, the external B-field can be applied in an arbitrary orientation, though for the field along y , λ_2 remains constant, which can be of particular interest.

CONCLUSIONS

The time dependence of the magnetization of the two endofullerene SMMs $Dy_2S@C_{82}$ and $Tb_2ScN@C_{80}$ at sub-Kelvin temperatures is revisited and used to extract quantum tunneling rates of the magnetization which lie in the GHz range. The proposed model completes the description of the ground state, is robust and can be applied to any coupled anisotropic 4f ion pair. While all states have no magnetic moment in zero field, the ground state displays a nonlinearly increasing magnetic moment in applied magnetic fields. These findings facilitate the search for quantum behavior in such systems if coherent tunneling of the magnetization shall be explored and exploited.

AUTHOR INFORMATION

Corresponding Author

Thomas Greber – Physik-Institut, Universität Zürich, CH-8057 Zürich, Switzerland; orcid.org/0000-0002-5234-1937; Email: greber@physik.uzh.ch

Complete contact information is available at: <https://pubs.acs.org/10.1021/acsomega.4c04388>

Notes

The author declares no competing financial interest.

ACKNOWLEDGMENTS

Financial support from the Swiss National Science Foundation (SNF project 201086) is gratefully acknowledged. The author

has benefited from discussions with Hans-Benjamin Braun, and Ari P. Seitsonen designed Figure 1a,b.

REFERENCES

- Heitler, W.; London, F. Wechselwirkung neutraler Atome und homöopolare Bindung nach der Quantenmechanik. *Zeitschrift für Physik* **1927**, *44*, 455–472.
- Gordon, J. P.; Zeiger, H. J.; Townes, C. H. Molecular Microwave Oscillator and New Hyperfine Structure in the Microwave Spectrum of NH_3 . *Phys. Rev.* **1954**, *95*, 282–284.
- Khomitsky, D. V.; Studenikin, S. A. Single-spin Landau-Zener-Stückelberg-Majorana interferometry of Zeeman-split states with strong spin-orbit interaction in a double quantum dot. *Phys. Rev. B* **2022**, *106*, 195414.
- Thomas, L.; Lioni, F.; Ballou, R.; Gatteschi, D.; Sessoli, R.; Barbara, B. Macroscopic quantum tunnelling of magnetization in a single crystal of nanomagnets. *Nature* **1996**, *383*, 145–147.
- Gatteschi, D.; Sessoli, R.; Villain, J. *Molecular Nanomagnets*; Oxford University Press: 2006.
- Giraud, R.; Wernsdorfer, W.; Tkachuk, A.; Maily, D.; Barbara, B. Nuclear spin driven quantum relaxation in $LiY_0.998Ho_0.002F_4$. *Phys. Rev. Lett.* **2001**, *87*, 057203.
- Luis, F.; Mettes, F.; Evangelisti, M.; Morello, A.; de Jongh, L. Approach of single-molecule magnets to thermal equilibrium. *J. Phys. Chem. Solids* **2004**, *65*, 763–771.
- Bartolomé, E.; Arauzo, A.; Luzón, J.; Bartolomé, J.; Bartolomé, F. In *Chapter 1 - Magnetic Relaxation of Lanthanide-Based Molecular Magnets*; Brück, E., Ed.; Handbook of Magnetic Materials; Elsevier: 2017; Vol. 26; pp 1–289.
- Yin, B.; Li, C.-C. A method to predict both the relaxation time of quantum tunneling of magnetization and the effective barrier of magnetic reversal for a Kramers single-ion magnet. *Phys. Chem. Chem. Phys.* **2020**, *22*, 9923–9933.
- Ishikawa, N.; Sugita, M.; Ishikawa, T.; Koshihara, S.; Kaizu, Y. Lanthanide double-decker complexes functioning as magnets at the single-molecular level. *J. Am. Chem. Soc.* **2003**, *125*, 8694–8695.
- Guo, F.-S.; Day, B. M.; Chen, Y.-C.; Tong, M.-L.; Mansikkamaki, A.; Layfield, R. A. Magnetic hysteresis up to 80 K in a dysprosium metalloocene single-molecule magnet. *Science* **2018**, *362*, 1400–1403.
- Vincent, R.; Klyatskaya, S.; Ruben, M.; Wernsdorfer, W.; Balestro, F. Electronic read-out of a single nuclear spin using a molecular spin transistor. *Nature* **2012**, *488*, 357–360.
- Godfrin, C.; Ferhat, A.; Ballou, R.; Klyatskaya, S.; Ruben, M.; Wernsdorfer, W.; Balestro, F. Operating Quantum States in Single Magnetic Molecules: Implementation of Grover's Quantum Algorithm. *Phys. Rev. Lett.* **2017**, *119*, 187702.
- Natterer, F. D.; Yang, K.; Paul, W.; Willke, P.; Choi, T.; Greber, T.; Heinrich, A. J.; Lutz, C. P. Reading and writing single-atom magnets. *Nature* **2017**, *543*, 226.
- Forrester, P. R.; Patthey, F.; Fernandes, E.; Sblendorio, D. P.; Brune, H.; Natterer, F. D. Quantum state manipulation of single atom magnets using the hyperfine interaction. *Phys. Rev. B* **2019**, *100*, 180405.
- Stevenson, S.; Rice, G.; Glass, T.; Harich, K.; Cromer, F.; Jordan, M. R.; Craft, J.; Hadju, E.; Bible, R.; Olmstead, M. M.; Maitra, K.; Fisher, A. J.; Balch, A. L.; Dorn, H. C. Small-bandgap endohedral metallofullerenes in high yield and purity. *Nature* **1999**, *401*, 55–57.
- Vieru, V.; Ungur, L.; Chibotaru, L. F. Key Role of Frustration in Suppression of Magnetization Blocking in Single-Molecule Magnets. *J. Phys. Chem. Lett.* **2013**, *4*, 3565–3569.
- Westerström, R.; Dreiser, J.; Piamonteze, C.; Muntwiler, M.; Weyeneth, S.; Krämer, K.; Liu, S.-X.; Decurtins, S.; Popov, A.; Yang, S.; Dunsch, L.; Greber, T. Tunneling, remanence, and frustration in dysprosium-based endohedral single-molecule magnets. *Phys. Rev. B* **2014**, *89*, 060406.
- Rinehart, J. D.; Long, J. R. Exploiting single-ion anisotropy in the design of f-element single-molecule magnets. *Chem. Sci.* **2011**, *2*, 2078–2085.

(20) Cimpoesu, F.; Dragoe, N.; Ramanantoanina, H.; Umland, W.; Daul, C. The theoretical account of the ligand field bonding regime and magnetic anisotropy in the DySc₂N@C₈₀ single ion magnet endohedral fullerene. *Phys. Chem. Chem. Phys.* **2014**, *16*, 11337–11348.

(21) Briganti, M.; Lucaccini, E.; Chelazzi, L.; Ciattini, S.; Sorace, L.; Sessoli, R.; Totti, F.; Perfetti, M. Magnetic Anisotropy Trends along a Full 4f-Series: The fn+7 Effect. *J. Am. Chem. Soc.* **2021**, *143*, 8108–8115.

(22) Zhang, Y.; Krylov, D.; Rosenkranz, M.; Schiemenz, S.; Popov, A. A. Magnetic anisotropy of endohedral lanthanide ions: paramagnetic NMR study of MSc₂N@C₈₀-Ih with M running through the whole 4f row. *Chem. Sci.* **2015**, *6*, 2328–2341.

(23) Dunsch, L.; Yang, S.; Zhang, L.; Svitova, A.; Oswald, S.; Popov, A. A. Metal Sulfide in a C₈₂ Fullerene Cage: A New Form of Endohedral Clusterfullerenes. *J. Am. Chem. Soc.* **2010**, *132*, 5413–5421.

(24) Nakao, K.; Kurita, N.; Fujita, M. Ab initio molecular-orbital calculation for C₇₀ and seven isomers of C₈₀. *Phys. Rev. B* **1994**, *49*, 11415–11420.

(25) Krylov, D.; Velkos, G.; Chen, C.-H.; Büchner, B.; Kostanyan, A.; Greber, T.; Avdoshenko, S. M.; Popov, A. A. Magnetic hysteresis and strong ferromagnetic coupling of sulfur-bridged Dy ions in clusterfullerene Dy₂S@C₈₂. *Inorg. Chem. Front.* **2020**, *7*, 3521–3532.

(26) Kostanyan, A.; Westerström, R.; Kunhardt, D.; Büchner, B.; Popov, A. A.; Greber, T. Sub-Kelvin hysteresis of the dilanthanide single-molecule magnet Tb₂ScN@C₈₀. *Phys. Rev. B* **2020**, *101*, 134429.

(27) Westerström, R.; Dubrovin, V.; Junghans, K.; Schlesier, C.; Büchner, B.; Avdoshenko, S. M.; Popov, A. A.; Kostanyan, A.; Dreiser, J.; Greber, T. Precise measurement of angles between two magnetic moments and their configurational stability in single-molecule magnets. *Phys. Rev. B* **2021**, *104*, 224401.

(28) Yang, W.; Velkos, G.; Liu, F.; Sudarkova, S. M.; Wang, Y.; Zhuang, J.; Zhang, H.; Li, X.; Zhang, X.; Büchner, B.; Avdoshenko, S. M.; Popov, A. A.; Chen, N. Single Molecule Magnetism with Strong Magnetic Anisotropy and Enhanced Dy–Dy Coupling in Three Isomers of Dy-Oxide Clusterfullerene Dy₂O@C₈₂. *Adv. Sci.* **2019**, *6*, 1901352.

(29) Chen, C.-H.; Krylov, D. S.; Avdoshenko, S.; Liu, F.; Spree, L.; Yadav, R.; Alvertis, A.; Hozoi, L.; Nenkov, K.; Kostanyan, A.; Greber, T.; Wolter, A. U. B.; Popov, A. A. Selective arc-discharge synthesis of Dy₂S-clusterfullerenes and their isomer-dependent single molecule magnetism. *Chem. Sci.* **2017**, *8*, 6451–6465.

(30) Thiele, S.; Vincent, R.; Holzmann, M.; Klyatskaya, S.; Ruben, M.; Balestro, F.; Wernsdorfer, W. Electrical Readout of Individual Nuclear Spin Trajectories in a Single-Molecule Magnet Spin Transistor. *Phys. Rev. Lett.* **2013**, *111*, 037203.

(31) Moreno-Pineda, E.; Taran, G.; Wernsdorfer, W.; Ruben, M. Quantum tunnelling of the magnetisation in single-molecule magnet isotopologue dimers. *Chem. Sci.* **2019**, *10*, 5138–5145.

(32) Flores Gonzalez, J.; Pointillart, F.; Cador, O. Hyperfine coupling and slow magnetic relaxation in isotopically enriched DyIII mononuclear single-molecule magnets. *Inorg. Chem. Front.* **2019**, *6*, 1081–1086.